Spontaneous breaking of rotational symmetry in rotating solitons: A toy model of excited nucleons with high angular momentum

Itay Hen* and Marek Karliner+

Raymond and Beverly Sackler School of Physics and Astronomy, Tel-Aviv University, Tel-Aviv 69978, Israel

(Received 10 March 2008; published 9 June 2008)

We study the phenomenon of spontaneous breaking of rotational symmetry in the rotating solutions of two types of baby Skyrme models. In the first, the domain is a two-sphere, and in the other, the Skyrmions are confined to the interior of a unit disk. Numerical full-field results show that when the angular momentum of the Skyrmions increases above a certain critical value, the rotational symmetry of the solutions is broken and the minimal-energy configurations become less symmetric. We propose a possible mechanism as to why spontaneous breaking of rotational symmetry is present in the rotating solutions of these models, while it is not observed in the ''usual'' baby Skyrme model. Our results might be relevant for a qualitative understanding of the nonspherical deformation of excited nucleons with high orbital angular momentum.

DOI: 10.1103/PhysRevD.77.116002 PACS numbers: 05.45.Yv, 03.50.−z, 14.20.Dh

I. INTRODUCTION

The phenomenon of spontaneous breaking of rotational symmetry (SBRS) in rotating systems relates to occurrences in which physical systems which rotate fast enough deform in a manner which breaks their rotational symmetry, a symmetry which is present when these systems are static or rotating slowly. The recognition that rotating physical systems can yield solutions with less symmetry than the governing equations is not new. One famous example which dates back to 1834 is that of the equilibrium configurations of a rotating fluid mass. It was Jacobi who was first to discover that, if rotated fast enough, a self-gravitating fluid mass can have equilibrium configurations lacking rotational symmetry. In modern terminology, Jacobi's asymmetric equilibria appear through a symmetry-breaking bifurcation from a family of symmetric equilibria as the angular momentum of the system increases above a critical value (a ''bifurcation point'') [1,2]. Above this critical value, rotationally symmetric configurations are no longer stable, and configurations with a broken rotational symmetry become energetically favorable.

By now it is widely recognized that symmetry-breaking bifurcations in rotating systems are of frequent occurrence and that this is in fact a very general phenomenon, appearing in a variety of physical settings among which are fluid dynamics, star formation, heavy nuclei, chemical reactions, plasmas, and biological systems, to mention some diverse examples.

Recently, SBRS has also been observed in self-gravitating N-body systems [3,4], where the equilibrium configurations of an N-body self-gravitating system enclosed in a finite three-dimensional spherical volume have been investigated using a mean-field approach. It was shown that when the ratio of the angular momentum of the system to its energy is high, spontaneous breaking of rotational symmetry occurs, manifesting itself in the formation of double-cluster structures. These results have also been confirmed with direct numerical simulations [5].

It is well known that a large number of phenomena exhibited by many-body systems have their counterparts and parallels in field theory, which in some sense is a limiting case of N-body systems in the limit $N \to \infty$. Since the closest analogies to a lump of matter in field theories are solitons, the presence of SBRS in self-gravitating N-body systems has led us to expect that it may also be present in solitonic field theories.

Our main motivation towards studying SBRS in solitons is that in hadronic physics Skyrme-type solitons [6] often provide a fairly good qualitative description of nucleon properties. In particular, it is interesting to ask what happens when such solitons rotate quickly, because this might shed some light on the nonspherical deformation of excited nucleons with high orbital angular momentum, a subject which is now of considerable interest. We address this issue in more detail in the concluding section of this manuscript.

In what follows, we study SBRS in one of the simplest and well-known field theoretic models admitting stable rotating solitonic solutions, namely, the baby Skyrme model [7,8]. First, we give a brief account for the occurrence of SBRS in physical systems in general, and then use the insights gained from this discussion to infer the conditions under which SBRS might appear in solitonic models and, in that context, study its appearance in baby Skyrme models. Specifically, we shall show that SBRS emerges if the domain manifold of the model is a two-sphere or a disk, while if the domain is $\mathbb{R}^2$, SBRS does not occur.

*itayhe@post.tau.ac.il
+marek@proton.tau.ac.il

II. SBRS FROM A DYNAMICAL POINT OF VIEW

The onset of SBRS may be qualitatively understood as resulting from a competition between the static energy of a system and its moment of inertia. To see this, let us consider a system described by a set of degrees of freedom ϕ, and assume that the dynamics of the system is governed by a Lagrangian which is invariant under spatial rotations. When the system is static, its equilibrium configuration is obtained by minimizing its static energy E_{static} with respect to its degrees of freedom ϕ,

$$\frac{\delta E}{\delta \phi} = 0 \quad \text{where } E = E_{\text{static}}(\phi). \tag{1}$$

Usually, if $E_{\text{static}}(\phi)$ does not include terms which manifestly break rotational symmetry, the solution to (1) is rotationally symmetric (with the exception of degenerate spontaneously broken vacua, which are not of our concern here). If the system rotates with a given angular momentum $\boldsymbol{J} = J\hat{z}$, its configuration is naturally deformed. Assuming that the Lagrangian of the system is quadratic in the time derivatives, stable rotating configurations (if such exist) are obtained by minimizing its total energy E_J,

$$\frac{\delta E_J}{\delta \phi} = 0 \quad \text{where } E_J = E_{\text{static}}(\phi) + \frac{J^2}{2I(\phi)}, \tag{2}$$

where $I(\phi)$ is the ratio between the angular momentum of the system and its angular velocity $\boldsymbol{\omega} = \omega\hat{z}$ (which for simplicity we assume is oriented in the direction of the angular momentum). $I(\phi)$ is the (scalar) moment of inertia of the system.

The energy functional (2) consists of two terms. The first, E_{static}, increases with the asymmetry. This is simply a manifestation of the minimal-energy configuration in the static case being rotationally symmetric. The second term $J^2/2I$, having the moment of inertia in the denominator, decreases with the asymmetry. At low values of angular momentum, the E_{static} term dominates, and thus asymmetry is not energetically favorable, but as the value of angular momentum increases, it is the second term which becomes dominant, thus giving rise to a possible breaking of rotational symmetry.

A. The self-gravitating ellipsoid

As an illustration of the above reasoning, let us consider the simple problem of a self-gravitating ellipsoid of liquid mass M [9]. The density of the ellipsoid ρ is assumed to be constant but its shape is allowed to deform. The boundary of the ellipsoid may be parametrized by

$$r(\theta, \varphi) = \left(\eta^2 \cos^2\theta + \frac{4\pi\rho}{3M}\frac{\sin^2\theta}{\eta(1-\epsilon^2)} \times (1 + \epsilon^2 - 2\epsilon\cos 2\varphi)\right)^{-1/2}, \tag{3}$$

with $\theta \in [0, \pi]$ being the polar angle and $\varphi \in [0, 2\pi)$ the azimuthal angle. Here, the ellipsoid has 2 degrees of freedom, $\phi = (\eta, \epsilon)$, with a third degree of freedom eliminated by the constraint of constant volume, and a nonzero value of ϵ indicates breaking of rotational symmetry. The static energy of the ellipsoid is due to self-gravitation and is given by

$$E_{\text{static}}(\eta, \epsilon) = -\frac{3}{10}GM^2 \int_0^\infty ((a_1 + u)(a_2 + u) \times (a_3 + u))^{-1/2} \mathrm{d}u, \tag{4}$$

where $a_1 = \frac{3M\eta}{4\pi\rho}\frac{1+\epsilon}{1-\epsilon}$, $a_2 = \frac{3M\eta}{4\pi\rho}\frac{1-\epsilon}{1+\epsilon}$, and $a_3 = 1/\eta^2$ [1]. The minimal-energy configuration of the static self-gravitating ellipsoid is obtained by minimizing (4) with respect to the parameters η and ϵ, giving

$$\eta = \left(\frac{4\pi\rho}{3M}\right)^{1/3}, \qquad \epsilon = 0 \rightarrow r(\theta, \varphi) = 1/\eta. \tag{5}$$

This means that the configuration that minimizes E_{static} is a sphere. When the ellipsoid is rotated with angular momentum $\boldsymbol{J} = J\hat{z}$, the expression for its energy becomes

$$E_J = E_{\text{static}}(\eta, \epsilon) + \frac{J^2}{2I(\eta, \epsilon)}, \tag{6}$$

where $I(\eta, \epsilon)$ is the moment of inertia of the ellipsoid

$$I(\eta, \epsilon) = \frac{3M^2\eta}{10\pi\rho}\frac{1+\epsilon^2}{1-\epsilon^2}. \tag{7}$$

Note that both $E_{\text{static}}(\eta, \epsilon)$ and $I(\eta, \epsilon)$ are monotonically increasing functions of the symmetry-breaking parameter ϵ, as discussed earlier. It is the "competition" between these two expressions in the minimization of (6) that determines whether and when SBRS occurs.

A (numerical) minimization of the energy functional (6) for different values of J with respect to the parameters η and ϵ (the constants of the problem are taken to be

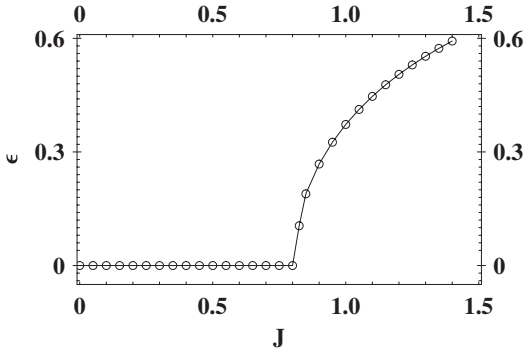

FIG. 1. The self-gravitating ellipsoid ($M = \frac{4}{3}\pi$, $\rho = 1$, and $GM^2 = 5/3$): the "symmetry-breaking" parameter ϵ for the minimal-energy configuration as a function of the angular momentum J, showing the existence of a critical angular momentum $J_{\text{crit}} \approx 0.8$ above which the ellipsoid is no longer axially symmetric. The line is to guide the eye.

$M = \frac{4}{3}\pi$, $\rho = 1$, and $GM^2 = 5/3$) indeed reveals the presence of SBRS. Below a critical value of angular momentum J_{crit} (which here is $J_{\text{crit}} \approx 0.8$), axially symmetric configurations are energetically more favorable, and $\epsilon = 0$ minimizes the energy; the ellipsoid boundary is an oblate spheroid. Above J_{crit}, however, the energy functional is no longer minimized by $\epsilon = 0$ and bifurcation occurs; the minimal-energy configurations become ellipsoids with three unequal axes. These results are summarized in Fig. 1.

III. SBRS IN BABY SKYRME MODELS

In what follows, we show that the above mechanism of SBRS is present in solitonic field theories as well, specifically in certain types of baby Skyrme models.

The baby Skyrme model is a nonlinear theory in $(2 + 1)$ dimensions which has several applications in condensed-matter physics [10]. The target manifold is a three-dimensional vector $\boldsymbol{\phi}$ with the constraint $\boldsymbol{\phi} \cdot \boldsymbol{\phi} = 1$. The Lagrangian density is given by

$$\mathcal{L} = \frac{1}{2}\partial_\mu \boldsymbol{\phi} \cdot \partial^\mu \boldsymbol{\phi} - \frac{\kappa^2}{2}[(\partial_\mu \boldsymbol{\phi} \cdot \partial^\mu \boldsymbol{\phi})^2 - (\partial_\mu \boldsymbol{\phi} \cdot \partial_\nu \boldsymbol{\phi}) \cdot (\partial^\mu \boldsymbol{\phi} \cdot \partial^\nu \boldsymbol{\phi})] - \mu^2(1 - \phi_3), \quad (8)$$

equipped with a Minkowski metric. The first term in the Lagrangian is the usual kinetic term known from σ models. The second term is fourth order in derivatives and is the analogue of the Skyrme term in the $(3 + 1)D$ Skyrme model [11,12]. The last term is a potential term, which is introduced to ensure the stability of the solutions [13]. Henceforth, we shall refer to this model as the ''usual'' or ''original'' baby Skyrme model.

The existence of stable solutions in this model is a consequence of the nontrivial topology of the mapping $\mathcal{M}$ of the physical space into the field space at a given time, $\mathcal{M}$: $\mathbb{R}^2 \mapsto S^2$, where the physical space $\mathbb{R}^2$ is compactified to S^2 by requiring the spatial infinity to be equivalent in each direction. The topology which stems from this one-point compactification allows the classification of maps into equivalence classes, each of which has a unique conserved quantity called the topological charge.

The static solutions of the baby Skyrme model (8) have rotationally symmetric energy and charge distributions in the charge-one and charge-two sectors [7]. The charge-one Skyrmion has an energy peak at its center which drops down exponentially. The energy distribution of the charge-two Skyrmion has a ringlike peak around its center at some characteristic distance. The rotating solutions of the model have also been previously studied [8,14]. It has been found that rotation at low angular velocities slightly deforms the Skyrmion, but it remains rotationally symmetric. For larger values of angular velocity, the rotationally symmetric configuration becomes unstable, but in this case the Skyrmion does not undergo symmetry breaking. Its stability is restored through a different mechanism, namely, that of radiation. The Skyrmion radiates out the excessive energy and angular momentum and, as a result, begins slowing down until it reaches equilibrium at some constant angular velocity, its core remaining rotationally symmetric. Moreover, if the Skyrme fields are restricted to a rotationally symmetric (hedgehog) form, the critical angular velocity above which the Skyrmion radiates can be obtained analytically. It is simply the coefficient of the potential term $\omega_{\text{crit}} = \mu$ [8]. Numerical full-field simulations we have conducted show that the Skyrmion actually begins radiating well below ω_{crit}, as radiation itself may be non-rotationally symmetric. The Skyrmion's core, however, remains rotationally symmetric for every angular velocity.

The stabilizing effect of the radiation on the solutions of the model has led us to believe that models in which radiation is somehow inhibited may turn out to be good candidates for the occurrence of SBRS. In the present paper we study two such baby Skyrme models. In these models energy and angular momentum are not allowed to escape to infinity through radiation, and for high enough angular momentum the mechanism responsible for SBRS discussed in the previous section takes over, revealing solutions with spontaneously broken rotational symmetry.

The first model we discuss is a baby Skyrme model in which the physical space $\mathbb{R}^2$ is replaced by a unit two-sphere, and in the second model Skyrmions are confined to the inside of a unit circle in $\mathbb{R}^2$. We compute the minimal-energy configurations of the rotating solutions of both models by applying a full-field relaxation method with which exact numerical solutions are obtained. For the baby Skyrme model on the two-sphere we also take a more analytical approach using rational maps. We discuss these models and the minimization method in more detail in the next section.

IV. THE BABY SKYRME MODEL ON THE TWO-SPHERE

The first baby Skyrme model we investigate which exhibits SBRS is the one for which both the domain and target manifolds are unit two-spheres. This model may be thought of as Skyrme's original 3D model once the radial coordinate is integrated out [15]. As in the usual baby Skyrme model, the Lagrangian density is simply

$$\mathcal{L} = \frac{1}{2}\partial_\mu \boldsymbol{\phi} \cdot \partial^\mu \boldsymbol{\phi} - \frac{\kappa^2}{2}[(\partial_\mu \boldsymbol{\phi} \cdot \partial^\mu \boldsymbol{\phi})^2 - (\partial_\mu \boldsymbol{\phi} \cdot \partial_\nu \boldsymbol{\phi})(\partial^\mu \boldsymbol{\phi} \cdot \partial^\nu \boldsymbol{\phi})], \quad (9)$$

with the metric $ds^2 = dt^2 - d\theta^2 - \sin^2\theta d\varphi^2$, where θ is the polar angle $\in [0, \pi]$ and φ is the azimuthal angle $\in [0, 2\pi)$. In this model a potential term is not necessary for the stability of the solutions [15] and thus is omitted. The Lagrangian of this model is invariant under rotations in both the domain and the target spaces, possessing an $O(3)_{\text{domain}} \times O(3)_{\text{target}}$ symmetry.

As in the original baby Skyrme model, the relevant homotopy group here is $\pi_2(S^2) = \mathbb{Z}$, implying that each field configuration is characterized by an integer topological charge B, the topological degree of the map $\boldsymbol{\phi}$, which in spherical coordinates is given by

$$B = \frac{1}{4\pi}\int \mathrm{d}\Omega \frac{\boldsymbol{\phi}\cdot(\partial_\theta\boldsymbol{\phi}\times\partial_\varphi\boldsymbol{\phi})}{\sin\theta}, \tag{10}$$

where $\mathrm{d}\Omega = \sin\theta \mathrm{d}\theta\mathrm{d}\varphi$. Static solutions within each topological sector are obtained by minimizing the energy functional

$$E_{\mathrm{static}} = \frac{1}{4\pi B}\int \mathrm{d}\Omega\Big(\frac{1}{2}(\partial_\theta\boldsymbol{\phi})^2 + \frac{1}{2}\frac{1}{\sin^2\theta}(\partial_\varphi\boldsymbol{\phi})^2 + \frac{\kappa^2}{2}\frac{(\partial_\theta\boldsymbol{\phi}\times\partial_\varphi\boldsymbol{\phi})^2}{\sin^2\theta}\Big), \tag{11}$$

where the $(4\pi B)^{-1}$ factor has been inserted for convenience. The static solutions of the model were studied in detail in [15] up to charge $B = 14$. These which are rotationally symmetric are the charge-one Skyrmion which has an analytic ''hedgehog'' solution with spherically symmetric energy and charge distributions, and the charge-two solution which has an axially symmetric ringlike solution.

In order to find the stable rotating solutions of the model, we assume for simplicity that any stable solution would rotate around the axis of angular momentum (which is taken to be the z direction) with some angular velocity ω. The rotating solutions thus take the form $\boldsymbol{\phi}(\theta, \varphi, t) = \boldsymbol{\phi}(\theta, \varphi - \omega t)$. The energy functional to be minimized is

$$E = E_{\mathrm{static}} + \frac{J^2}{2I}, \tag{12}$$

where I is the ratio of the angular momentum of the Skyrmion to its angular velocity, or its ''moment of inertia,'' given by

$$I = \frac{1}{4\pi B}\int \mathrm{d}\Omega((\partial_\varphi\boldsymbol{\phi})^2 + \kappa^2(\partial_\theta\boldsymbol{\phi}\times\partial_\varphi\boldsymbol{\phi})^2). \tag{13}$$

A. The numerical procedure

Since the Euler-Lagrange equations derived from the energy functional (12) are nonlinear *partial differential equations*, in general the minimal-energy configurations can only be obtained with the aid of numerical techniques. In what follows, we obtain the minimal-energy configurations which correspond to rotating Skyrmion solutions, using a full-field relaxation method, in which the domain S^2 is discretized to a spherical grid—100 grid points for θ and 100 points for φ. The relaxation process begins by initializing the field triplet $\boldsymbol{\phi}$ to a rotationally symmetric configuration,

$$\boldsymbol{\phi}_{\mathrm{initial}} = (\sin\theta\cos B\varphi, \sin\theta\sin B\varphi, \cos\theta), \tag{14}$$

where B is the topological charge of the Skyrmion in question. The energy of the baby Skyrmion is then minimized by repeating the following steps: a point (θ_m, φ_n) on the grid is chosen at random, along with one of the three components of the field $\boldsymbol{\phi}(\theta_m, \varphi_n)$. The chosen component is then shifted by a value δ_ϕ chosen uniformly from the segment $[-\Delta_\phi, \Delta_\phi]$ where $\Delta_\phi = 0.1$ initially. The field triplet is then normalized and the change in energy is calculated. If the energy decreases, the modification of the field is accepted and otherwise it is discarded. The procedure is repeated while the value of Δ_ϕ is gradually decreased throughout the procedure. This is done until no further decrease in energy is observed.

One undesired feature of this minimization scheme is that it can get stuck at a local minimum. This problem can be resolved by using the ''simulated annealing'' algorithm [16,17], which in fact has been successfully implemented before, in obtaining the minimal-energy configurations of static two- and three-dimensional Skyrmions [18]. The algorithm is comprised of repeated applications of a Metropolis algorithm with a gradually decreasing temperature, based on the fact that when a physical system is slowly cooled down, reaching thermal equilibrium at each temperature, it will end up in its ground state. This algorithm, however, is much more expensive in terms of computer time. We therefore employ it only on a representative sample of the parameter space, just as a check on our results, which correspond to a Metropolis algorithm of zero temperature.

B. Results

In what follows we present the results obtained by the minimization scheme described in the previous section to the rotating solutions of the model in the charge-one and charge-two sectors, which as mentioned above are rotationally symmetric. For simplicity, we fix the parameter κ at $\kappa^2 = 0.01$, although other κ values were tested as well, yielding qualitatively similar solutions.

1. Rotating charge-one solutions

In perfect analogy with the self-gravitating ellipsoid discussed in the Introduction, the rotating charge-one Skyrmion, which has spherically symmetric energy and charge distributions in the static limit [Fig. 2(a)], was found to exhibit SBRS. When rotated slowly, its symmetry is reduced to $O(2)$, with the axis of symmetry coinciding with the axis of rotation [Fig. 2(b)]. At some critical value of angular momentum (which in the current settings is $J_{\mathrm{crit}} \approx 0.2$), the axial symmetry is further broken, yielding an ellipsoidal energy distribution with three unequal axes [Fig. 2(c)]. Any further increase in angular momentum results in the elongation of the Skyrmion in one horizontal direction and its shortening in the perpendicular one. The results are very similar to those of the rotating self-gravitating ellipsoid.

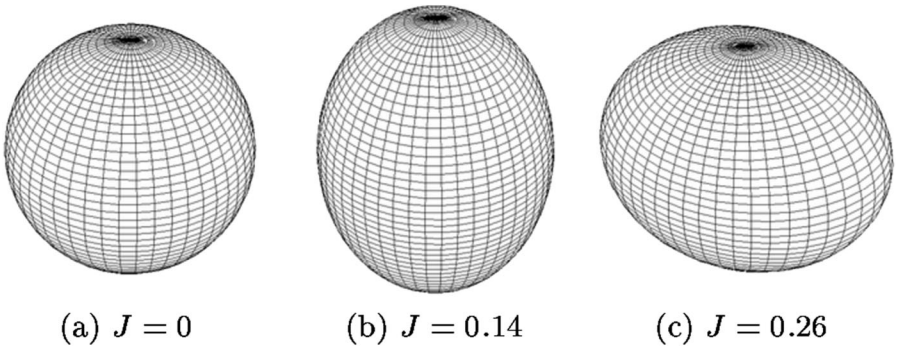

FIG. 2. Baby Skyrmions on the two-sphere ($\kappa^2 = 0.01$): the charge distribution $\mathcal{B}(\theta, \varphi)$ of the charge-one Skyrmion for different angular momenta. In the figure, the vector $\mathcal{B}(\theta, \varphi)\hat{\boldsymbol{r}}$ is plotted for the various θ and φ values.

2. Rotating charge-two solutions

SBRS is also observed in rotating charge-two Skyrmions. The static charge-two Skyrmion has only axial symmetry [Fig. 3(a)], with its symmetry axis having no preferred direction. Nonzero angular momentum aligns the axis of symmetry with the axis of rotation. For small values

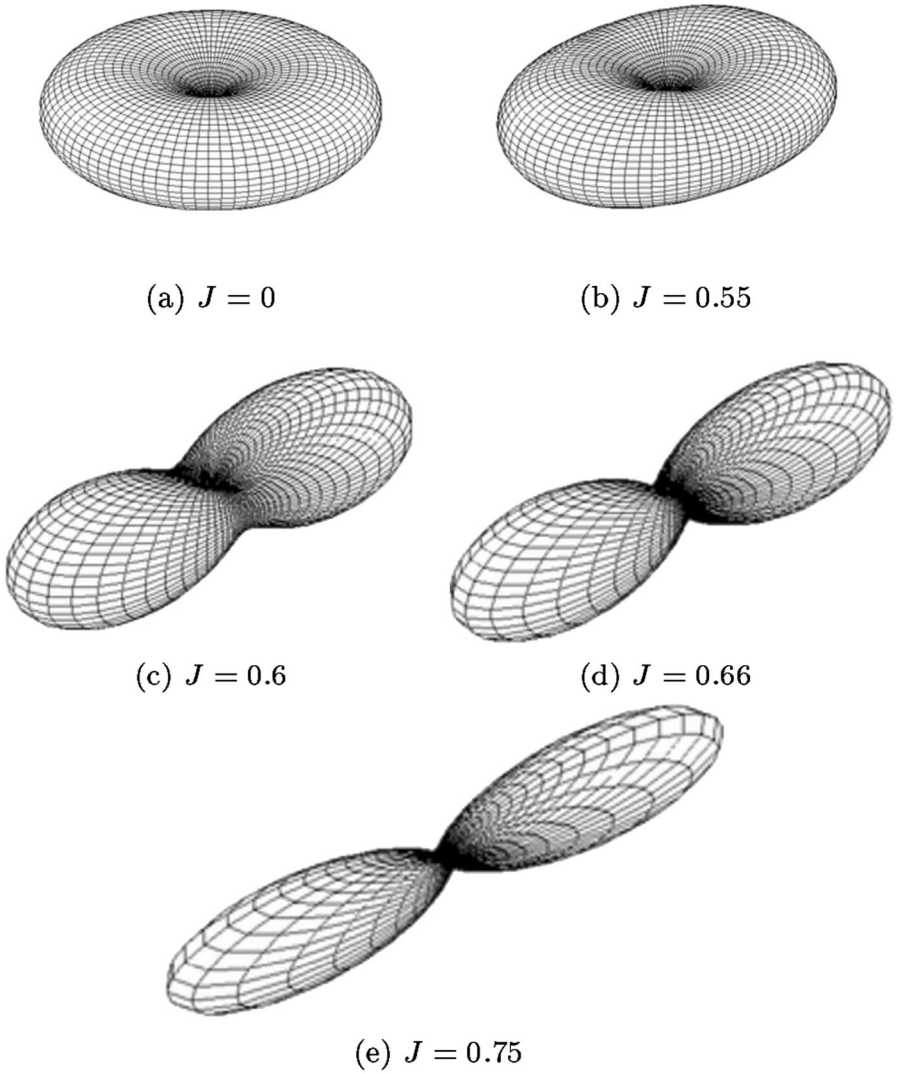

FIG. 3. Baby Skyrmions on the two-sphere ($\kappa^2 = 0.01$): the charge distribution $\mathcal{B}(\theta, \varphi)$ of the charge-two Skyrmion for different angular momenta. In the figure, the vector $\mathcal{B}(\theta, \varphi)\hat{\boldsymbol{r}}$ is plotted for the various θ and φ values.

of angular momentum, the Skyrmion is slightly deformed but remains axially symmetric [Fig. 3(b)]. Above $J_{\text{crit}} \approx 0.55$, however, its rotational symmetry is broken, and it starts splitting to its "constituent" charge-one Skyrmions [Figs. 3(c) and 3(d)]. As the angular momentum is further increased, the splitting becomes more evident, and the Skyrmion assumes a stringlike shape. This is somewhat reminiscent of the well-known elongation, familiar from high-spin hadrons which are also known to assume a stringlike shape with the constituent quarks taking position at the ends of the string [19,20].

A quantitative measure for the deviation from rotational symmetry of the rotating solutions may be obtained by evaluating the expression

$$\Delta^2 = \int\left(\frac{1}{2B}\int \mathcal{B}(\theta,\varphi)\sin\theta d\theta\right)^2 \frac{d\varphi}{2\pi} - 1, \tag{15}$$

where $\mathcal{B}(\theta,\varphi)$ is the charge density of the Skyrmion. For rotationally symmetric configurations $\Delta = 0$. In Fig. 4, Δ is plotted against the angular momentum J, for both the charge-one and the charge-two solutions. The qualitative similarity to the bifurcation occurring in the rotating liquid mass system shown in Fig. 1 is clear.

C. The rational map ansatz

A somewhat more analytical analysis of this system may be achieved by the use of the rational maps approximation scheme [21], which is known to provide quite accurate results for the static solutions of the model [15]. In this approximation, points on the base sphere are expressed by the Riemann coordinate $z = \tan\frac{\theta}{2}e^{i\varphi}$, and the ansatz for the field triplet is

$$\boldsymbol{\phi} = \left(\frac{R+\bar{R}}{1+|R|^2}, i\frac{R-\bar{R}}{1+|R|^2}, \frac{1-|R|^2}{1+|R|^2}\right), \tag{16}$$

where the complex-valued function $R(z)$ is a rational map of degree B between Riemann spheres,

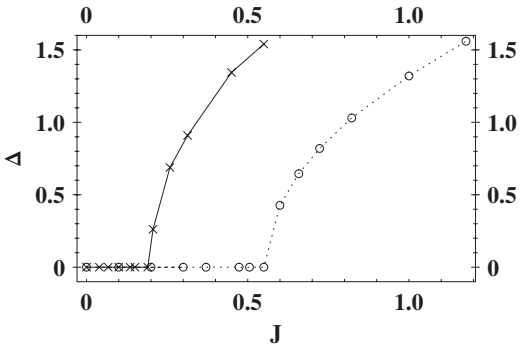

FIG. 4. The deviation from rotational symmetry Δ of the rotating charge-one (denoted by $\times$) and charge-two (denoted by $\circ$) Skyrmions for different values of angular momentum. The lines are to guide the eye.

$$R(z) = \frac{p(z)}{q(z)}. \tag{17}$$

Here, $p(z)$ and $q(z)$ are polynomials in z, such that $\max[\deg(p), \deg(q)] = B$, and p and q have no common factors. Rational maps of degree B correspond to field configurations with charge B.

In its implementation here, we have simplified matters even more and reduced the degrees of freedom of the maps by a restriction only to those maps which exhibit the symmetries observed in the rotating full-field solutions. This allowed the isolation of those parameters which are the most critical for the minimization of the energy functional.

As shown in Fig. 2, the charge and energy densities of the charge-one Skyrmion exhibit progressively lower symmetries as J is increased. The static solution has an $O(3)$ symmetry, while the slowly rotating solution has an $O(2)$ symmetry. Above a certain critical J, the $O(2)$ symmetry is further broken and only an ellipsoidal symmetry survives. Rational maps of degree one, however, cannot produce charge densities which have all the discrete symmetries of an ellipsoid with three unequal axes. Nonetheless, approximate solutions with only a reflection symmetry through the xy plane (the plane perpendicular to the axis of rotation) and a reflection through one horizontal axis may be generated by the following one-parametric family of rational maps:

$$R(z) = \frac{\cos\alpha}{z + \sin\alpha}, \tag{18}$$

which has the charge density

$$\mathcal{B}(\theta,\varphi) = \left(\frac{\cos\alpha}{1+\sin\alpha\sin\theta\cos\varphi}\right)^2. \tag{19}$$

Here, $\alpha \in [-\pi, \pi]$ is the parameter of the map, with $\alpha = 0$ corresponding to a spherically symmetric solution and a nonzero value of α corresponding to a nonrotationally symmetric solution. Results of a numerical minimization of the energy functional (12) for fields constructed from (18) for different values of angular momentum J are shown in Fig. 5(a). While for angular momentum less than $J_{\text{crit}} \approx 0.1$, $\alpha = 0$ minimizes the energy functional (a spherically symmetric solution), above this critical value bifurcation occurs and $\alpha = 0$ is no longer a minimum; the rotational symmetry of the charge-one Skyrmion is broken and it becomes nonrotationally symmetric.

A similar analysis of the charge-two rotating solution yields the one-parametric map

$$R(z) = \frac{\sin\alpha + z^2\cos\alpha}{\cos\alpha + z^2\sin\alpha}, \tag{20}$$

with corresponding charge density

$$\mathcal{B}(\theta,\varphi) = \left(\frac{2\cos 2\alpha\sin\theta}{2+\sin^2\theta(\sin 2\alpha\cos 2\varphi - 1)}\right)^2. \tag{21}$$

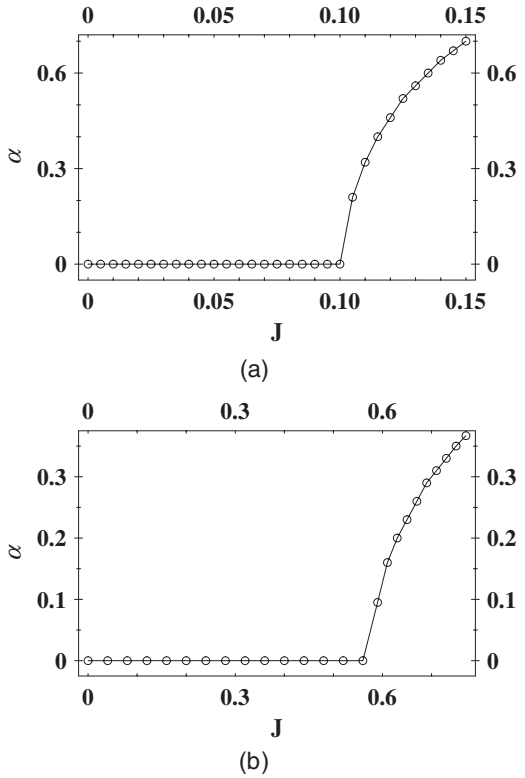

FIG. 5. Spontaneous breaking of rotational symmetry in the restricted rational maps approximation for the baby Skyrmions on the two-sphere: the parameter α as a function of the angular momentum J, for the charge-one (top panel) and the charge-two (bottom panel) solutions. The lines are to guide the eye.

In this case, $\alpha = 0$ corresponds to a toroidal configuration, and a nonzero value of α yields solutions very similar to those shown in Fig. 3, having the proper discrete symmetries. The results in this case are summarized in Fig. 5(b), indicating that above $J_{\text{crit}} \approx 0.57$ the minimal-energy configuration is no longer axially symmetric.

The discrepancies in the critical angular momenta J_{crit} between the full-field method (0.2 for charge-one and 0.55 for charge-two) and the rational maps scheme (0.1 for charge-one and 0.57 for charge-two) are of course expected, as in the latter method the solutions have only 1 degree of freedom. Nonetheless, the qualitative similarity in the behavior of the solutions in both cases is strong.

V. THE BABY SKYRME MODEL ON A DISK

A second model in which SBRS is observed is a baby Skyrme model for which radiation is inhibited by confining the Skyrmion to the inside of a unit circle. The domain $\mathbb{R}^2$ of the usual baby Skyrme model is replaced by the unit disk

$$D^2 = \{\boldsymbol{x} \in \mathbb{R}^2 : |\boldsymbol{x}|^2 \leq 1\}. \tag{22}$$

To recover the topology necessary for the existence of nontrivial solutions, we require that the fields are the same in each direction on the bounding unit circle. This results in the domain D^2 becoming topologically equivalent to a two-sphere, and the topological charge is now given by the expression

$$B = \frac{1}{4\pi} \int_{D^2} \mathrm{d}r\mathrm{d}\varphi \boldsymbol{\phi} \cdot (\partial_r \boldsymbol{\phi} \times \partial_\varphi \boldsymbol{\phi}), \tag{23}$$

where r and φ are the usual polar coordinates. As in the usual baby Skyrme model, the static solutions are found by minimizing the static energy functional

$$E_{\text{static}} = \frac{1}{4\pi B} \int_{D^2} r\mathrm{d}r\mathrm{d}\varphi \left(\frac{1}{2} \left(\partial_r \boldsymbol{\phi} \cdot \partial_r \boldsymbol{\phi} + \frac{1}{r^2} \partial_\varphi \boldsymbol{\phi} \cdot \partial_\varphi \boldsymbol{\phi} \right) + \frac{\kappa^2}{2} \frac{(\partial_r \boldsymbol{\phi} \times \partial_\varphi \boldsymbol{\phi})^2}{r^2} + \mu^2 (1 - \phi_3) \right), \tag{24}$$

where the integration is over the unit disk, and the rotating solutions are equivalently obtained by minimizing the functional

$$E_{\text{J}} = E_{\text{static}} + \frac{J^2}{2I}, \tag{25}$$

where as before I is the moment of inertia:

$$I = \frac{1}{4\pi B} \int_{D^2} r\mathrm{d}r\mathrm{d}\theta (\partial_\varphi \boldsymbol{\phi} \cdot \partial_\varphi \boldsymbol{\phi} + \kappa^2 (\partial_r \boldsymbol{\phi} \times \partial_\varphi \boldsymbol{\phi})^2). \tag{26}$$

The numerical minimization of the energy functional has been carried out using the relaxation method discussed earlier in the case of the baby Skyrme model on the two-sphere, and the parameters of the model were fixed at $\mu^2 = 1$ and $\kappa^2 = 0.01$ for simplicity.

Here we focused our attention on the charge-one and charge-two Skyrmions, as in the static limit these are found to be rotationally symmetric with the form

$$\boldsymbol{\phi}(r, \theta) = (\sin f(r) \cos B\varphi, \sin f(r) \sin B\varphi, \cos f(r)), \tag{27}$$

where the profile function $f(r)$ satisfies the boundary conditions $f(0) = \pi$ and $f(1) = 0$. Figure 6 shows the profile function obtained for each of the charges.

As in the baby Skyrme model on the two-sphere, spontaneous breaking of rotational symmetry is observed in this

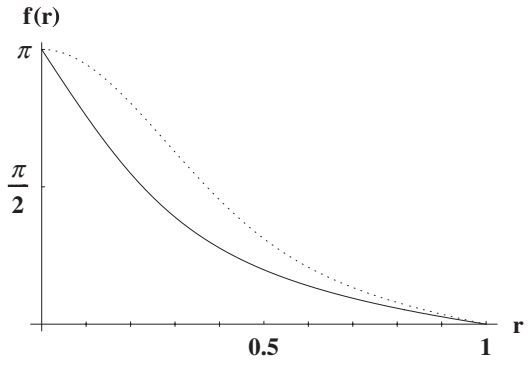

FIG. 6. The baby Skyrme model on a disk ($\mu^2 = 1$ and $\kappa^2 = 0.01$): profile functions of the static charge-one (solid line) and charge-two (dotted line) Skyrmions.

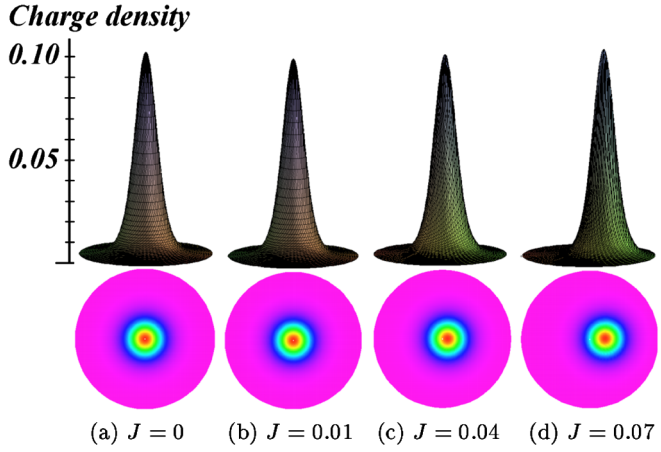

FIG. 7 (color online). Top: The charge density of the charge-one Skyrmion for different values of the angular momentum. Bottom: Corresponding contour plots ranging from violet (low density) to red (high density). Above $J \approx 0.03$, the minimal-energy configurations are no longer rotationally symmetric; the center of mass of the Skyrmion is slightly shifted towards the bounding circle.

model as well. In the charge-one sector, below $J \approx 0.03$ the stable solutions are rotationally symmetric with only slight deformations from the static shape. Above this value SBRS appears; the Skyrmion's center of mass shifts towards the bounding circle. This is summarized in Fig. 7. A similar situation occurs for the charge-two Skyrmions. The critical value there is $J \approx 0.14$ as illustrated in Fig. 8. The behavior of the rotating solutions may be understood as follows: by moving away from the center of the circle, the moment of inertia of the Skyrmion increases as dictated by Steiner's theorem. Since its shape remains more or less the same, its ''self-energy'' stays relatively unaffected (this is more evident in the charge-one case).

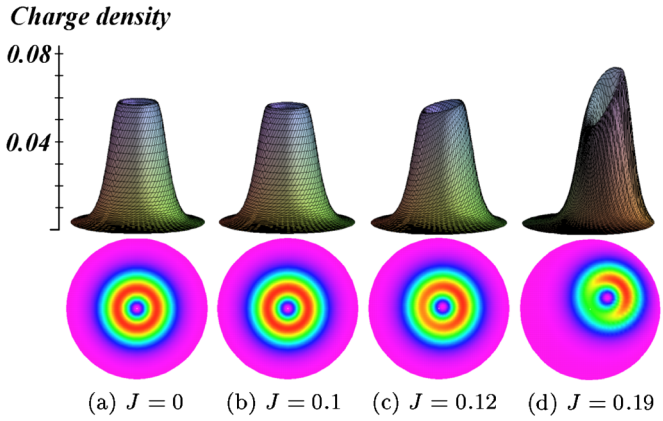

FIG. 8 (color online). Top: The charge density of the charge-two Skyrmion for different values of the angular momentum. Bottom: Corresponding contour plots ranging from violet (low density) to red (high density). Above $J \approx 0.11$, the minimal-energy configurations are no longer rotationally symmetric.

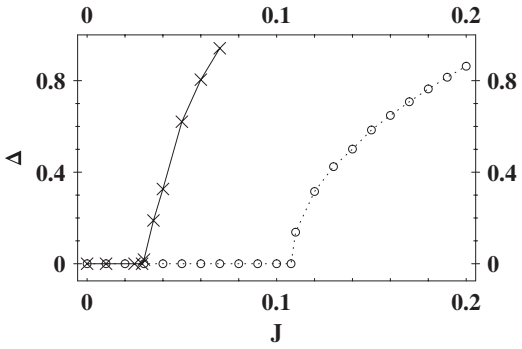

FIG. 9. The baby Skyrme model on a disk: the symmetry-breaking measure Δ as a function of the angular momentum for the charge-one (denoted by $\times$) and the charge-two (denoted by $\circ$) Skyrmions.

As with the baby Skyrmions on the two-sphere, the deviation from rotational symmetry is measured by

$$\Delta^2 = \int \left(\frac{1}{2B} \int \mathcal{B}(r, \varphi) r \mathrm{d}r \right)^2 \frac{\mathrm{d}\varphi}{2\pi} - 1, \qquad (28)$$

with $\mathcal{B}(r, \varphi)$ being the charge density of the Skyrmion. In Fig. 9, Δ is plotted as a function of the angular momentum, showing the emergence of SBRS as bifurcation points at the critical values of angular momentum.

VI. SUMMARY AND FURTHER REMARKS

In this work we have studied SBRS in two solitonic models whose solutions exhibit SBRS when the angular momentum is sufficiently high. We have shown that the emergence of SBRS in these models can be directly linked to its appearance in classical mechanical systems, such as the rotating liquid mass, and that this linkage originates from general principles, and hence points out the universality of this phenomenon.

We believe that the results obtained in the present work may, at least to some extent, also be linked to recent advances in understanding the nonsphericity of excited nucleons with large orbital momentum. Nonspherical deformation of the nucleon shape is now a focus of considerable interest, both experimentally [22,23] and theoretically [24–26]. As Skyrmions are known to provide a good qualitative description of many nucleon properties, we hope that the results presented here will provide some corroboration to recent results on this subject, e.g., [26], although a more detailed analysis of this analogy is in order. We hope to be able to report on these matters in forthcoming publications.

ACKNOWLEDGMENTS

This work was supported in part by a grant from the Israel Science Foundation administered by the Israel Academy of Sciences and Humanities.

[1] R. A. Lyttleton, *The Stability of Rotating Liquid Masses* (Cambridge University Press, Cambridge, England, 1953).
[2] S. Chandrasekhar, *Ellipsoidal Figures of Equilibrium* (Yale University Press, New Haven, CT, 1969).
[3] E. V. Votyakov, H. I. Hidmi, A. DeMartino, and D. H. E. Gross, Phys. Rev. Lett. **89**, 031101 (2002).
[4] E. V. Votyakov, A. DeMartino, and D. H. E. Gross, Eur. Phys. J. B **29**, 593 (2002).
[5] M. Karliner, Proceedings of the London Mathematical Society Durham Symposium, http://www.maths.dur.ac.uk/events/Meetings/LMS/2004/TSA/Movies/Karliner.wmv, 2004.
[6] For a review of Skyrmion physics see, e.g., I. Zahed and G. E. Brown, Phys. Rep. **142**, 1 (1986); G. Holzwarth and B. Schwesinger, Rep. Prog. Phys. **49**, 825 (1986).
[7] B. M. A. G. Piette, B. J. Schoers, and W. J. Zakrzewski, Z. Phys. C **65**, 165 (1995).
[8] B. M. A. G. Piette, B. J. Schoers, and W. J. Zakrzewski, Nucl. Phys. **B439**, 205 (1995).
[9] A different approach to the more general problem of a self-gravitating liquid mass of an arbitrary shape can be found in [1].
[10] A. A. Belavin and A. M. Polyakov, JETP Lett. **22**, 245 (1975).
[11] T. H. R. Skyrme, Proc. R. Soc. A **260**, 127 (1961).
[12] T. H. R. Skyrme, Nucl. Phys. **31**, 556 (1962).
[13] The exact form of the potential in the baby Skyrme Lagrangian may be chosen almost arbitrarily, but we shall use the given potential as a reference case.
[14] M. Betz, H. B. Rodrigues, and T. Kodama, Phys. Rev. D **54**, 1010 (1996).
[15] I. Hen and M. Karliner, Phys. Rev. E **77**, 036612 (2008).
[16] S. Kirkpatrick, C. D. Gellat, and M. P. Vecchi, Science **220**, 671 (1983).
[17] S. Geman and D. Geman, IEEE Transactions on Pattern Analysis and Machine Intelligence **6**, 721 (1984).
[18] M. Hale, O. Schwindt, and T. Weidig, Phys. Rev. E **62**, 4333 (2000).
[19] Y. Nambu, Phys. Rev. D **10**, 4262 (1974).
[20] J. S. Kang and H. J. Schnitzer, Phys. Rev. D **12**, 841 (1975).
[21] C. J. Houghton, N. S. Manton, and P. M. Sutcliffe, Nucl. Phys. **B510**, 507 (1998).
[22] M. K. Jones *et al.*, Phys. Rev. Lett. **84**, 1398 (2000).
[23] O. Gayou *et al.*, Phys. Rev. Lett. **88**, 092301 (2002).
[24] G. A. Miller, Phys. Rev. C **68**, 022201(R) (2003).
[25] A. Kvinikhidze and G. A. Miller, Phys. Rev. C **73**, 065203 (2006).
[26] G. A. Miller, Phys. Rev. C **76**, 065209 (2007).